

Article

The Influence of Seasonal Variability of Eutrophication Indicators on Carbon Dioxide and Methane Diffusive Emissions in the Largest Shallow Urban Lake in China

Bingjie Ma, Yang Wang, Ping Jiang and Siyue Li * 

School of Environmental Ecology and Biological Engineering, Institute of Changjiang Water Environment and Ecological Security, Hubei Key Laboratory of Novel Reactor and Green Chemical Technology, Wuhan Institute of Technology, Wuhan 430205, China; mabingjie6@163.com (B.M.); wangyang@wbpcas.cn (Y.W.); jp17856178727@163.com (P.J.)

* Correspondence: syli2006@163.com

Abstract: Eutrophication is prevalent in urban lakes; however, a knowledge gap exists regarding eutrophication influences on carbon dynamics in these ecosystems. In the present study, we investigated the carbon dioxide (CO₂) and methane (CH₄) concentration and diffusion fluxes in Lake Tangxun (the largest shallow Chinese urban lake) in the autumn and winter of 2022 and spring and summer of 2023. We found that Lake Tangxun served as a source of GHGs, with average emission rates of 5.52 ± 12.16 mmol CO₂ m⁻² d⁻¹ and 0.83 ± 2.81 mmol CH₄ m⁻² d⁻¹, respectively. The partial pressure of dissolved CO₂ (*p*CO₂) (averaging 1321.39 ± 1614.63 μatm) and dissolved CH₄ (*d*CH₄) (averaging 4.29 ± 13.71 μmol L⁻¹) exceeded saturation levels. Seasonal variability was observed in the *p*CO₂ and *d*CH₄ as well as CH₄ fluxes, while the CO₂ flux remained constant. The mean *p*CO₂ and *d*CH₄, as well as carbon emissions, were generally higher in summer and spring. *p*CO₂ and *d*CH₄ levels were significantly related to total nitrogen (TN), total phosphorus (TP), and ammonium-nitrogen (N-NH₄⁺), and N-NH₄⁺ was a main influencing factor of *p*CO₂ and *d*CH₄ in urban eutrophic lakes. The positive relationships of *p*CO₂, *d*CH₄ and trophic state index highlighted that eutrophication could elevate CO₂ and CH₄ emissions from the lake. This study highlights the fact that eutrophication can significantly increase carbon emissions in shallow urban lakes and that urban lakes are substantial contributors to the global carbon budget.

Keywords: eutrophication; urban lake; carbon dioxide; methane; greenhouse gases; diffusive flux



Citation: Ma, B.; Wang, Y.; Jiang, P.; Li, S. The Influence of Seasonal Variability of Eutrophication Indicators on Carbon Dioxide and Methane Diffusive Emissions in the Largest Shallow Urban Lake in China. *Water* **2024**, *16*, 136. <https://doi.org/10.3390/w16010136>

Academic Editor: Hucai Zhang

Received: 3 December 2023

Revised: 23 December 2023

Accepted: 25 December 2023

Published: 29 December 2023



Copyright: © 2023 by the authors. Licensee MDPI, Basel, Switzerland. This article is an open access article distributed under the terms and conditions of the Creative Commons Attribution (CC BY) license (<https://creativecommons.org/licenses/by/4.0/>).

1. Introduction

Lakes are an important component of inland water ecosystems and also hotspots of greenhouse gas (GHG), i.e., CO₂ and CH₄, release due to their high productivity and the exchange of material, energy, and information with terrestrial ecosystems [1–5]. Lacustrine CO₂ emission range from 0.11–0.57 Pg C yr⁻¹ [1,2,6,7]; likewise, lacustrine CH₄ evasion estimates vary even more widely, from 6 to 185 Tg CH₄ yr⁻¹ [8–11]. These research efforts underscore lakes as focal points for global carbon and CH₄ budgets, urging the need for meticulous investigation of lakes as a significant carbon source.

Urban lakes (normally with a mean depth of less than 3 m) are commonly shallow [12,13] and are indispensable components of landscape features and urban living environments [14,15]. Urban lakes have a vulnerability to a host of anthropogenic and environmental pressures and possess a poor capacity for self-purification [16]. Human activities, for instance, discharges of wastewater, can enhance loadings of organic carbon and nutrients in urban lakes, which can stimulate mineralization and thus promote methanogenesis [17]. Conversely, a surfeit of nutrients also enhances primary production, thereby increasing a lake's carbon sequestration capacity, and thus concurrently curtailing CO₂ emissions [18,19]. Beyond nutrients, environmental factors such as wind and temperature

also clearly affect urban lakes. Wind-induced turbulence, for instance, can reduce stratification and mitigate hypoxic conditions, thereby augmenting benthic oxygen availability and restraining CH₄ production, resulting in reduced CH₄ emissions and increasing CO₂ emissions [20,21]. Temperature, however, plays a multifaceted role, fostering primary production, which in turn can reduce CO₂ production [18,19]. However, studies exploring the characteristics and influencing factors of GHG emissions from urban lakes remain relatively scarce in the literature [22–24].

Eutrophication occurs widely in lakes and exerts a pivotal role in regulating GHG emissions from lakes [19,25,26]. It is worth noting that anthropogenic eutrophication is a predominant driver of lake eutrophication [27]. Studies have shown that eutrophic lakes can substantially enhance CH₄ production and emission [28,29]; however, the findings regarding CO₂ production and emission in eutrophic lakes are divergent. Some studies have demonstrated CO₂ emissions from eutrophic lakes to the atmosphere [25], yet others have reported a decrease in CO₂ emissions [19] or even a net CO₂ uptake from the atmosphere [30]. Notwithstanding the efforts made, the intricate web of CO₂ and CH₄ production and emission in response to lake eutrophication remains enigmatic and warrants further investigation. This knowledge gap represents the exigency for in-depth study to disentangle the nuances governing carbon in eutrophic lakes. As such, carbon exchange at the air–water interface, especially in eutrophic urban lakes, is an urgent imperative.

In the study, we used Lake Tangxun, the largest shallow urban lake located in a subtropical region, as an example to delve into the GHG dynamics of a eutrophic lake. The overarching objectives of our research endeavors were to (1) unravel the seasonal variation and driving factors in both the concentrations and fluxes of CO₂ and CH₄; (2) elucidate the profound effects of eutrophication on GHG dynamics in a shallow urban lake. We tested the hypotheses that (1) key drivers of seasonal fluctuations in GHGs concentrations and fluxes are variable, and (2) eutrophication considerably shapes the behavior of CO₂ and CH₄ in this specific lake ecosystem. The study aims to enhance our comprehension of GHG emissions in eutrophic shallow urban lakes, shedding light on informing effective mitigation strategy and management practice of lake carbon evasion, particularly within the context of escalating urbanization and its associated environmental challenges.

2. Materials and Methods

2.1. Study Area

Lake Tangxun (30°22′–30°30′ N, 114°15′–114°35′ E) is the largest Chinese urban lake. It lies in Wuhan, Hubei Province. Lake Tangxun includes an inner lake in the east, making up 33% of the total area, and an outer lake in the west (Figure 1). The water surface area and average depth of Lake Tangxun are 47.6 km² and 1.85 m, respectively [31,32]. Situated within a subtropical climatic zone, the lake is ice-free during winter months. The annual mean temperature and precipitation in the area are 18.3 °C (ranged –6–38 °C) and 1057.3 mm, respectively (Figure S1). The development of industry in the catchment area is a trajectory representing the onset of eutrophication in 1996 [31]. This evolution underscores the intricate interplay between urbanization environmental shifts, rendering Lake Tangxun a compelling natural laboratory for understanding eutrophication and its implications.

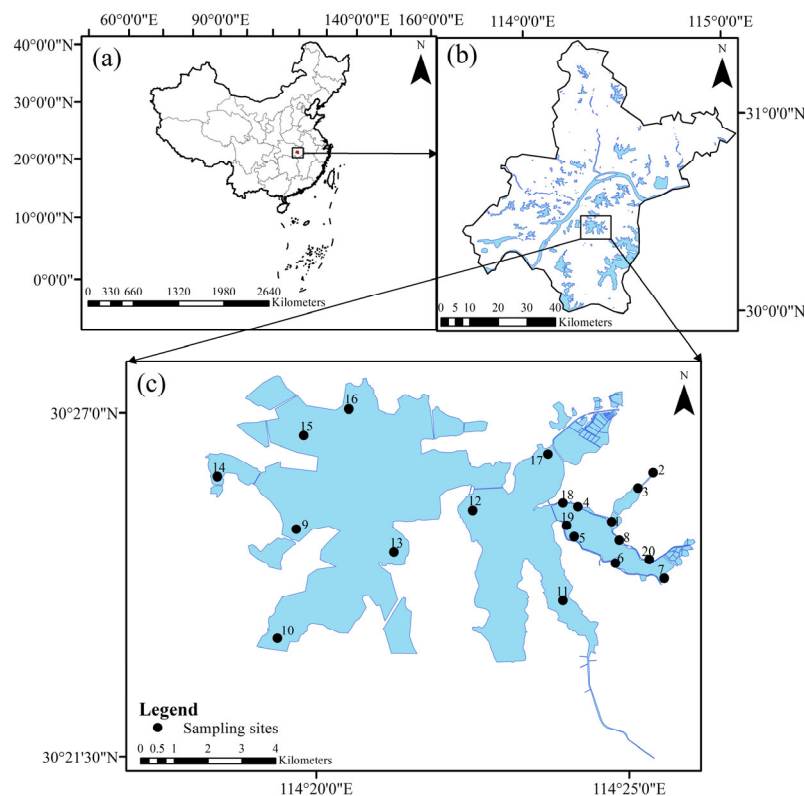


Figure 1. Locations and study sites of the Lake Tangxun (a–c). Numbers 1–20 are sampling sites.

2.2. Sample Collection and Measurements

Field sampling and surveys of Lake Tangxun were diligently executed in October 2022 and February, April, and June 2023. These temporal selections align with autumn, winter, spring, and summer, respectively. Twenty strategically designated sampling sites were meticulously selected in Lake Tangxun (Figure 1). This ensures the representativeness of our data collection. Site 1 is an aquaculture pond. Sites 2–3, 9–12, 15–18, and 20 are located near the sewage outlet; meanwhile, sites 9, 12, and 16 are the non-point source pollution catchments, and site 15 is in a village. Sites 4–8 and 19 are in Wetland Park. Sites 13 and 14 are campsites; additionally, site 14 also exists within a small amount of cropland. There is no seasonal variation in wastewater discharge, while rainfall runoff experiences seasonal variations [33]. It is noteworthy that no extreme hydrometeorological events were recorded during each sampling campaign, and the sampling as a whole represented the prevailing climatic and hydrological conditions in the region.

A Multi-Parameter Meter (Thermo Fisher Eutech, Singapore) was used to record the in situ surface water temperature (T_W), pH, electrical conductivity (EC) and dissolved oxygen (DO), with accuracies of ± 0.5 °C, ± 0.002 pH units, $\pm 1.0\%$ and $\pm 2.0\%$, respectively. A TES-1341 hot-wire anemometer (TES Corp., Taiwan, China) meter was used to record ambient temperature (T_a) and wind speed (U) about 1 m above overlying water, and a pressure probe recorded air pressure. Water samples (0.1–0.3 m beneath water surface) were gathered using a 2.5 L plexiglass hydrophore. Subsequently, water samples were filtered with pre-burnt glass fiber filter (0.7 μm pore size, Whatman, Maidstone, UK), and the filter membranes were used to measure chlorophyll a (Chl-a) via acetone extraction. Transparency (SD) was measured with a Secchi disk. All samples were placed in ice boxes in field and promptly preserved in refrigerators or subjected to freezing after reaching the lab.

Ultraviolet spectrophotometry (UV-8000, Shanghai Yuanxi Instrument Co., Ltd., Shanghai, China) can be applied to measure nutrient concentrations, including total nitrogen (TN), total phosphorus (TP), ammonium-nitrogen (N-NH_4^+), and nitrate-nitrogen (N-NO_3^-)

(<https://www.sac.gov.cn/> //, accessed on 1 November 2022). A TOC analyzer (Shimadzu, TOC-L, Kyoto, Japan) was used to analyze dissolved organic carbon (DOC).

The well-established headspace equilibrium method can directly measure CO₂ and CH₄ concentrations [34–36]. Seventy-mL water samples (0.1 m beneath water surface) were extracted via a 100 mL gas-tight syringe; subsequently a 30 mL volume of ambient atmosphere was extracted for equilibrating. The syringe was vigorously shaken to accelerate equilibrium. The resulting headspace gas samples were collected in a vacuum aluminum foil airbag (Delin Gas Packing Co., Ltd., Dalian, China). Meanwhile, ambient air was extracted at the overlying water. Gas samplings were analyzed with a gas chromatograph (Shimadzu, GC-2014, Kyoto, Japan). CO₂ and CH₄ concentrations were computed by Henry's law as follows [36]:

$$p\text{CO}_2 = C_G \times R \times T + V_g/V_w \times (C_{g-C} - C_{a-C}) \times K_{H-C} \quad (1)$$

$$d\text{CH}_4 = C_{g-M} \times K_{H-M} + V_g/V_w \times (C_{g-M} - C_{a-M}) \quad (2)$$

$$\ln K_{H-C} = -58.0931 + 90.5069 \times (100/T) + 22.2940 \times \ln (T/100) \quad (3)$$

$$K_{H-M} = \beta / 22.356 \quad (4)$$

$$\ln \beta = -68.8862 + 101.4956 \times (100/T) + 28.7314 \times \ln (T/100) \quad (5)$$

where $p\text{CO}_2$ is partial pressure of dissolved CO₂ (μatm); $d\text{CH}_4$ is dissolved CH₄ ($\mu\text{mol L}^{-1}$); C_{g-M} (or C_{g-C}) is the CH₄ (or CO₂) concentration of gas samples ($\mu\text{mol L}^{-1}$); T is measured T_W (K); R is prevalent gas constant ($0.082057 \text{ L atm mol}^{-1} \text{ K}^{-1}$); K_{H-M} (or K_{H-C}) is Henry solubility constant ($\text{mol L}^{-1} \text{ atm}^{-1}$) of CH₄ (or CO₂); V_g is the air volume and V_w is the water volume in balance (mL); C_{a-M} (or C_{a-C}) is atmospheric concentration of CH₄ (or CO₂) ($\mu\text{mol L}^{-1}$).

Theoretical diffusion model was used to calculate the gas diffusive fluxes (F , $\text{mmol m}^{-2} \text{ d}^{-1}$) as follows [37,38]:

$$F = k \times (C_w - C_a) \quad (6)$$

$$k = k_{600} \times (S_c/600)^{-n} \quad (7)$$

$$S_c(\text{CO}_2) = 1911.1 - 118.11 \times t + 3.4527 \times t^2 - 0.04132 \times t^3 \quad (8)$$

$$S_c(\text{CH}_4) = 1897.8 - 114.28 \times t + 3.2902 \times t^2 - 0.039061 \times t^3 \quad (9)$$

where k is the gas piston coefficient (cm h^{-1}); $(C_w - C_a)$ is concentration gradient ($\mu\text{mol L}^{-1}$). S_c is the Schmidt number regulated by water temperature (t , °C), the exponent n is a constant determined by measured wand speed, k_{600} is calculated using an empirical formula [39].

To elucidate the trophic status of Lake Tangxun and its effect on GHG dynamics, four major parameters were applied to calculate the trophic state index (TSI). TSI is calculated as follows [18]:

$$\text{TSI} = 0.219\text{TSI}(\text{TN}) + 0.230\text{TSI}(\text{TP}) + 0.326\text{TSI}(\text{Chl-a}) + 0.225\text{TSI}(\text{SDD}) \quad (10)$$

$$\text{TSI}(\text{TN}) = 10 \times (5.453 + 1.694 \times \ln\text{TN}) \quad (11)$$

$$\text{TSI}(\text{TP}) = 10 \times (9.436 + 1.624 \times \ln\text{TP}) \quad (12)$$

$$\text{TSI}(\text{Chl-a}) = 10 \times (2.5 + 1.086 \times \ln\text{Chl-a}) \quad (13)$$

$$\text{TSI}(\text{SDD}) = 10 \times (5.118 - 1.94 \times \ln\text{SD}) \quad (14)$$

where TSI values of 30–50, 50–60, 60–70 and >70 represent mesotrophic, eutrophic, moderately eutrophic and highly eutrophic, respectively.

2.3. Statistical Analyses

The substantial portion of the data were non-normal. The significant differences of the GHG concentrations and emissions, environmental parameters amongst seasons

were examined via Kruskal–Wallis test. A significance probability of $p < 0.05$ was used. Non-normal data are logarithmically transformed when necessary. Pearson’s correlation could explore relationships of gas concentration and physicochemical factors. IBM SPSS statistics 26 and Origin 2021 were used for statistical analyses. Origin 2021 was used for drawing figures.

3. Results

3.1. Environment Factors

Lake Tangxun showed substantial seasonal differences in physicochemical and biological properties (Figure 2). There were statistical differences in T_W , transparency, DO, EC, Chl-a, DOC, and $N\text{-NO}_3^-$ concentrations among seasons ($p < 0.001$); nevertheless, no statistical differences existed in U , pH, $N\text{-NH}_4^+$, TN or TP across seasons. The average T_W in winter (11.77 ± 1.53 °C) was significantly lower than in spring (26.28 ± 2.04 °C), summer (27.01 ± 1.55 °C), and autumn (21.04 ± 1.20 °C) (Figure 2a). The highest and lowest average of U and SD appeared in winter (1.33 ± 1.45 m s⁻¹ and 0.63 ± 0.22 m) and summer (0.76 ± 0.93 m s⁻¹ and 0.35 ± 0.16 m), respectively (Figure 2b,c).

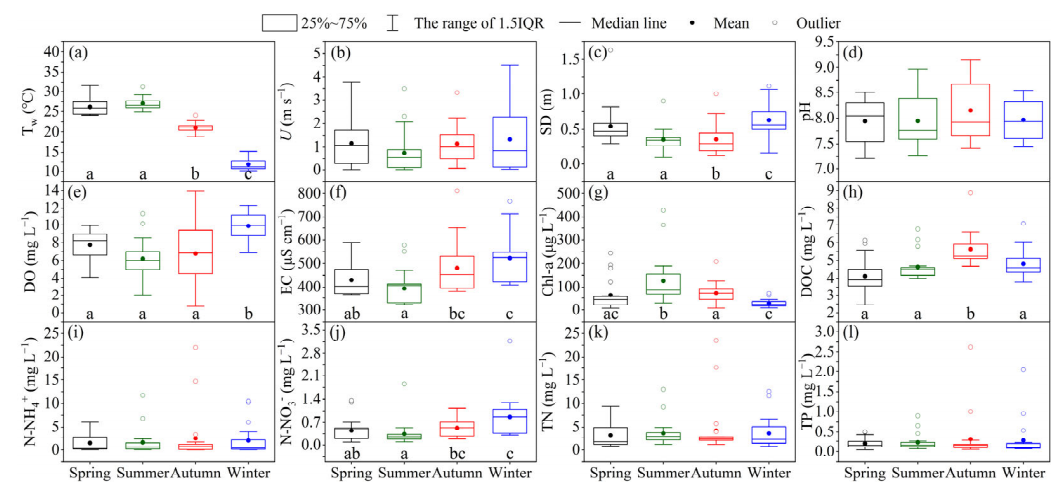


Figure 2. Seasonal variations of water quality in Lake Tangxun. (a) T_W ; (b) U ; (c) SD; (d) pH; (e) DO; (f) EC; (g) Chl-a; (h) DOC; (i) $N\text{-NH}_4^+$; (j) $N\text{-NO}_3^-$; (k) TN; (l) TP. Letters a, b and c denote significant differences among seasons.

The average pH value was slightly higher in autumn (8.14 ± 0.59) compared to the other seasons (Figure 2d). The DO concentrations and EC values firstly decreased and then increased (Figure 2e,f). They both were highest in winter (9.90 ± 1.45 mg L⁻¹ for DO and 522.60 ± 109.51 $\mu\text{S cm}^{-1}$ for EC, respectively) and lowest in summer (6.21 ± 2.27 mg L⁻¹ for DO and 394.00 ± 75.13 $\mu\text{S cm}^{-1}$ for EC, respectively). Inversely, the highest average Chl-a concentrations appeared in summer (125.81 ± 103.13 $\mu\text{g L}^{-1}$) and lowest appeared winter (27.78 ± 16.72 $\mu\text{g L}^{-1}$) (Figure 2g), respectively.

The mean concentrations of DOC, $N\text{-NH}_4^+$, TN, and TP first increased and then decreased (Figure 2h,i,k,l). The highest DOC (5.64 ± 0.93 mg L⁻¹), $N\text{-NH}_4^+$ (2.47 ± 5.62 mg L⁻¹), TN (4.25 ± 5.75 mg L⁻¹) and TP (0.31 ± 0.58 mg L⁻¹) were found in autumn but were lowest in spring (4.11 ± 0.99 mg L⁻¹, 1.44 ± 1.90 mg L⁻¹, 3.15 ± 2.56 mg L⁻¹ and 0.20 ± 0.14 mg L⁻¹, respectively). The highest average $N\text{-NO}_3^-$ concentration was in winter (0.87 ± 0.64 mg L⁻¹) and lowest in summer (0.35 ± 0.38 mg L⁻¹) (Figure 2j).

The TSI of Lake Tangxun showed a statistically significant difference among seasons ($p < 0.01$). The average TSI (67.68 ± 8.25) was less than 70, illustrating that the Lake Tangxun was a medial eutrophic lake overall (Figure 3). The pronounced seasonality in the TSI unveiled a highest value during the summer season (averaging 72.04 ± 6.77), but the lowest during the winter season (averaging 63.06 ± 6.91). Lake Tangxun was hypereutrophic in the summer, while it transitioned to a state of moderate eutrophication in the other seasons.

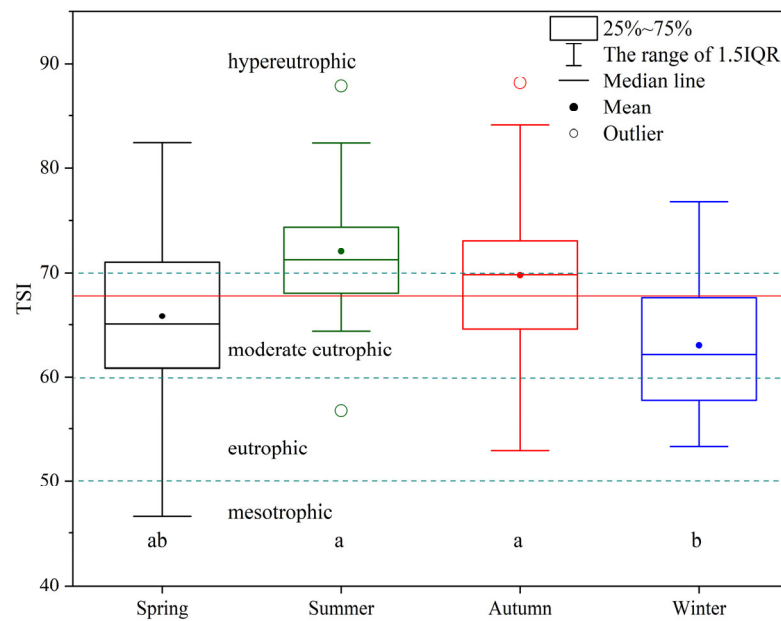


Figure 3. TSI seasonal variations in Lake Tangxun (non-parametric Kruskal–Wallis method). The trophic status was distinguished using green dotted lines and the red line represents the TSI mean. Letters a, b denote significant differences among seasons.

3.2. $p\text{CO}_2$ and CO_2 Flux

The mean $p\text{CO}_2$ is $1321.39 \pm 1614.63 \mu\text{atm}$ (range: 86–10,968 μatm). Of the measured $p\text{CO}_2$ data, 85% exceeded the atmospheric CO_2 average (526 μatm). The average $p\text{CO}_2$ in spring ($1621.50 \pm 1387.83 \mu\text{atm}$) and summer ($2217.91 \pm 2641.93 \mu\text{atm}$) was significantly higher than that in autumn ($647.71 \pm 172.21 \mu\text{atm}$) and in winter ($798.45 \pm 444.68 \mu\text{atm}$) ($p < 0.05$) (Figure 4a).

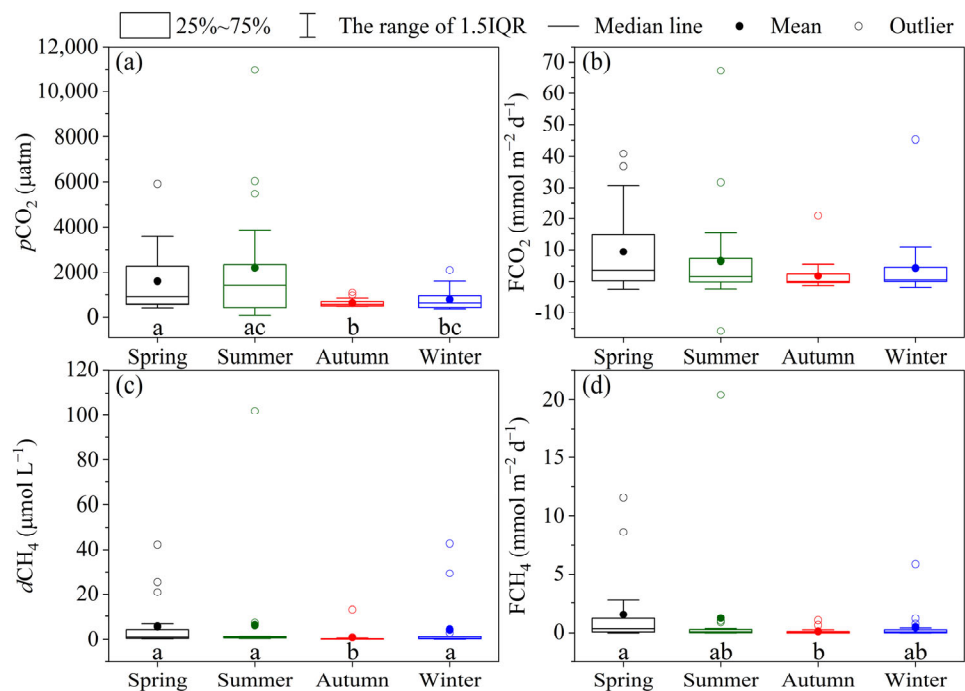


Figure 4. Seasonal variations in dissolved GHGs concentrations and diffusion fluxes in Lake Tangxun; (a,b) $p\text{CO}_2$ and FCO_2 among seasons; (c,d) $d\text{CH}_4$ and FCH_4 among seasons. Letters a, b and c denote significant differences among seasons.

The mean CO_2 flux is $5.52 \pm 12.16 \text{ mmol m}^{-2} \text{ d}^{-1}$ (range: $-15.83 - 67.30 \text{ mmol m}^{-2} \text{ d}^{-1}$). There was no significant difference amongst seasons (Figure 4b). The average CO_2 flux followed a decline trend as follows: spring ($9.36 \pm 13.10 \text{ mmol m}^{-2} \text{ d}^{-1}$) > summer ($6.49 \pm 16.88 \text{ mmol m}^{-2} \text{ d}^{-1}$) > winter ($4.39 \pm 10.17 \text{ mmol m}^{-2} \text{ d}^{-1}$) > autumn ($1.85 \pm 4.81 \text{ mmol m}^{-2} \text{ d}^{-1}$).

There were significant negative relationships of $p\text{CO}_2$ with pH, DO and Chl-a (Figure 5a–c). Additionally, $p\text{CO}_2$ had a strong positively relationship with N-NH_4^+ , TN, TP, and TSI (Figure 5d,f and Figure 6a).

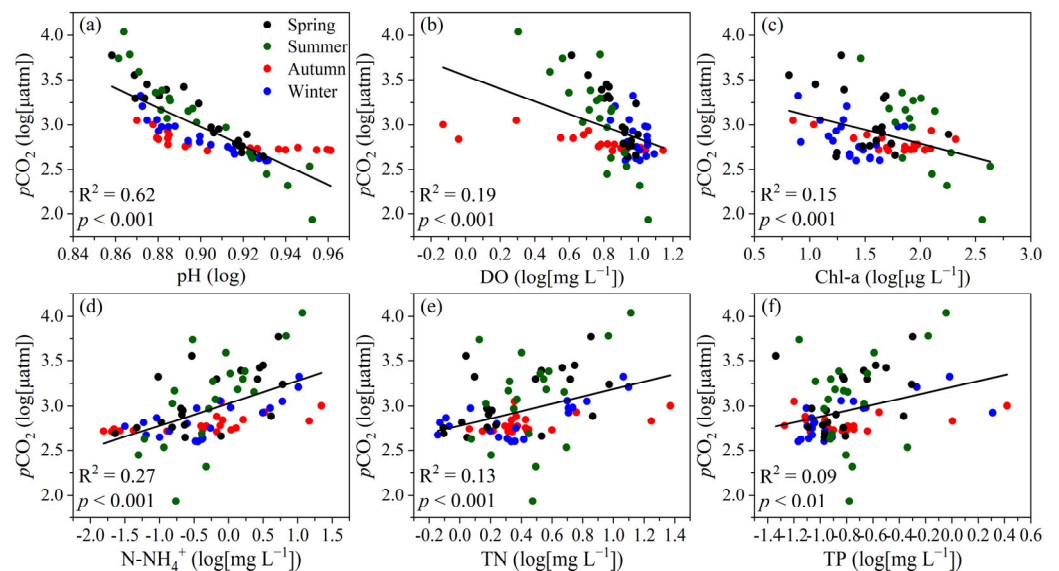


Figure 5. Relationship of $p\text{CO}_2$ with (a) pH; (b) DO; (c) Chl-a; (d) N-NH_4^+ ; (e) TN; (f) TP. R^2 and p values are shown.

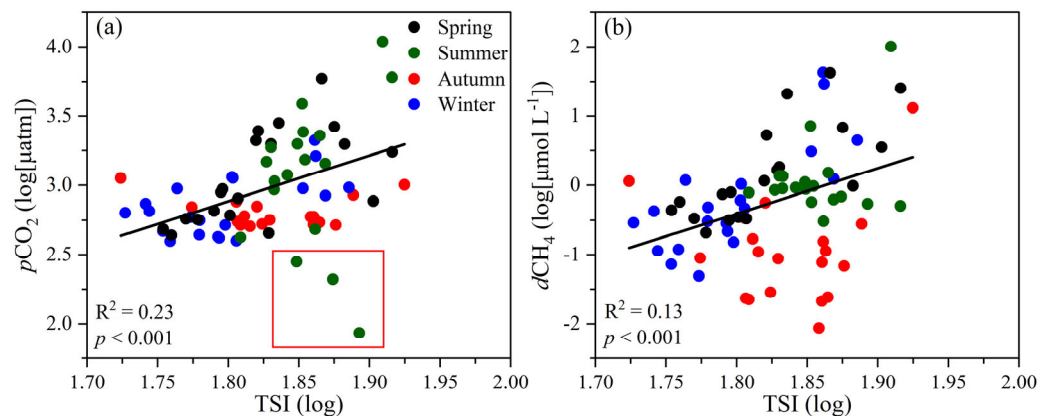


Figure 6. Relationship of TSI with (a) $p\text{CO}_2$ (after removing three outliers) and (b) $d\text{CH}_4$. R^2 and p values are shown. Solid circles in the red box represent outliers.

3.3. $d\text{CH}_4$ and CH_4 Flux

The overall $d\text{CH}_4$ changed between 0.01 and $102.00 \mu\text{mol L}^{-1}$ (mean: $4.29 \pm 13.71 \mu\text{mol L}^{-1}$). The mean value of atmospheric CH_4 concentration was $0.12 \pm 0.01 \mu\text{mol L}^{-1}$, illustrating oversaturation of CH_4 in Lake Tangxun. The mean $d\text{CH}_4$ in autumn ($0.83 \pm 2.90 \mu\text{mol L}^{-1}$) was lower than that in other seasons (spring: $5.74 \pm 11.01 \mu\text{mol L}^{-1}$, summer: $6.25 \pm 22.58 \mu\text{mol L}^{-1}$ and winter: $4.33 \pm 11.10 \mu\text{mol L}^{-1}$) ($p < 0.001$) (Figure 4c).

The overall CH_4 fluxes ranged between 5.48×10^{-5} and $20.42 \text{ mmol m}^{-2} \text{ d}^{-1}$, with a grand average of $0.83 \pm 2.81 \text{ mmol m}^{-2} \text{ d}^{-1}$. The average CH_4 flux followed a decline trend as follows: spring ($1.51 \pm 3.06 \text{ mmol m}^{-2} \text{ d}^{-1}$) was slightly higher than summer

($1.21 \pm 4.53 \text{ mmol m}^{-2} \text{ d}^{-1}$) and winter ($0.46 \pm 1.30 \text{ mmol m}^{-2} \text{ d}^{-1}$), and significantly higher than autumn ($0.13 \pm 0.25 \text{ mmol m}^{-2} \text{ d}^{-1}$) ($p < 0.05$) (Figure 4d).

$d\text{CH}_4$ exhibited significantly negative correlations with pH and DO (Figure 7a,b), while showed significantly positive correlations with N-NH_4^+ , TN and TP (Figure 7c–e). $d\text{CH}_4$ also revealed a significantly positive correlations with $p\text{CO}_2$ (Figure 7f) and TSI (Figure 6b).

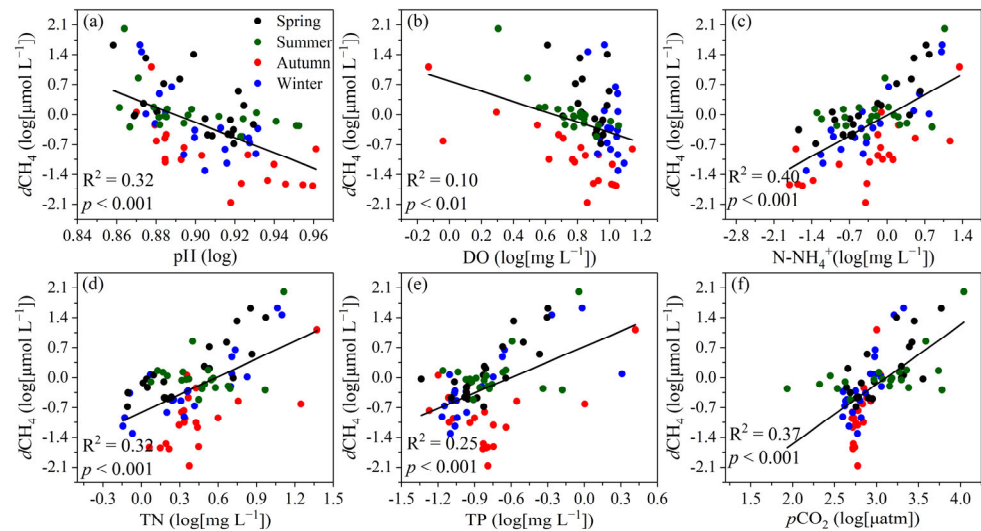


Figure 7. Linear regression of $d\text{CH}_4$ with (a) pH; (b) DO; (c) N-NH_4^+ ; (d) TN; (e) TP; (f) $p\text{CO}_2$. R^2 and p values are shown.

4. Discussion

4.1. Seasonal and Spatial Shifts of CO_2 and CH_4

We found clearly seasonal variations in $p\text{CO}_2$ with significantly higher average $p\text{CO}_2$ in spring and summer in Lake Tangxun ($p < 0.05$; Figure 4). This was attributable to the higher temperature and suitable precipitation in the two seasons (Figure S1). Higher temperature can increase in-site microorganism metabolism, and high temperature and precipitation promote heterotrophic respiration in the littoral soils; thus the surrounding soils have a higher CO_2 content, thereby transporting more CO_2 to lakes via runoff [34,40–42]. This was supported by the positive correlations of $p\text{CO}_2$ with T_a ($p < 0.01$) and precipitation ($p < 0.01$) (Figure S2).

Moreover, nutrient variables can favor in-stream respiration of DOC and photosynthetic up-taking of CO_2 ; this process can be responsible for the positive relationships between $p\text{CO}_2$ and nutrient elements of TN, TP and N-NH_4^+ , and the negative relationship between $p\text{CO}_2$ and Chl-a (Figure 5) [15,43].

The much lower $d\text{CH}_4$ observed in autumn (Figure 4c) was contrary to previous studies [19,44,45]. The authors ascribed this seasonal pattern to the synthetic effect of temperature and organic carbon availability [19,45,46]. Warmer temperatures can promote methanogenesis by affecting microbial metabolism [47], which can be confirmed by the remarked relationship between T_w and $d\text{CH}_4$ (Table S2). This can be ascribed to the faster decomposition rate of organic matter and consumption of dissolved oxygen at high temperatures, creating favorable conditions for methanogenesis, whilst frequent rain events in spring and summer (Figure S1) could potentially transport soil CH_4 into lakes and promote CH_4 diffusion from bottom to surface in lakes [48,49]. Moreover, although the highest mean DOC concentration occurred in autumn, internal respiration of organic carbon in autumn was lower than in winter, which can be confirmed by the correlation of DOC and $d\text{CH}_4$ (Table S2), resulting in $d\text{CH}_4$ in winter higher than that in autumn. We need to stress that seasonal variation of CH_4 dynamics was relatively complex in urban lakes.

We found that some points are significantly deviated from the average values (Figure 4), suggesting huge variability of data. The deviated values of $p\text{CO}_2$, $d\text{CH}_4$, CO_2 ,

and CH₄ diffusion fluxes are highly related to the environment characteristics of sampling points. The $p\text{CO}_2$ and $d\text{CH}_4$ were highly related to N-NH_4^+ , N-NO_3^- , and Chl-a (Table 1). The sites with deviated values of $p\text{CO}_2$ and $d\text{CH}_4$ exhibited higher N-NH_4^+ ; for instance, the highest concentrations of N-NH_4^+ and gases simultaneously occurred at site 20 (Table S1). CO_2 and CH_4 diffusion fluxes were not dependent on $p\text{CO}_2$ and $d\text{CH}_4$ but closely related to U (Figure S3). Random measures of wind speed could lead to CO_2 and CH_4 diffusion fluxes deviated from the average values at those sites with high wind speed.

Table 1. Stepwise regression with $p\text{CO}_2$ and $d\text{CH}_4$ and ambient conditions in Lake Tangxun. R^2 is adjust R^2 .

	CO_2	CH_4
Multiple regression	$p\text{CO}_2 = 2.61 + 0.29\text{N-NH}_4^+ - 0.23\text{N-NO}_3^- - 0.36\text{Chl-a} + 0.72T_w$	$d\text{CH}_4 = 2.00 + 0.41\text{N-NH}_4^+ - 0.89\text{N-NO}_3^- - 0.66\text{Chl-a} - 2.85\text{DOC} + 1.40\text{TN}$
R^2	0.44	0.59
p	<0.001	<0.001
Part R^2	0.27 ***, 0.05 *, 0.07 **, 0.05 **	0.40 *, 0.07 ***, 0.06 ***, 0.02 **, 0.04 **

Note: *, ** and *** represent $p < 0.05$, $p < 0.01$ and $p < 0.001$.

4.2. $p\text{CO}_2$ Control Factors

In-stream biogeochemical processes mainly control lake $p\text{CO}_2$ [50]. Chl-a can be a proxy of lacustrine primary productivity; thus, increasing Chl-a concentration can promote photosynthesis [29,30,34]. This photosynthetic process produces DO but consumes CO_2 , thereby resulting in the significant negative relationships of $p\text{CO}_2$ with Chl-a (Figure 5c), DO (Figure 5b), and pH (Figure 5a). Previous studies support the reciprocal relationships [26,51].

Nutrient loading can influence lake photosynthesis and bacterial respiration, thereby regulating $p\text{CO}_2$ in lakes [18,19]. For example, nutrients can favor both photosynthesis and in-site respiration of carbon. The decay of algae can add organic matter to the sediment and stimulate endogenous respiration in lakes [34]. In our studied lakes, lake-dissolved CO_2 is over-saturated, suggesting that the studied lakes are heterotrophic, thereby leading to the relationships of $p\text{CO}_2$ with N-NH_4^+ , TN, and TP (Figure 5d–f). The stepwise regression analysis model showed that N-NH_4^+ was a good predictor for estimating $p\text{CO}_2$ in Lake Tangxun (Table 1). N-NH_4^+ is a good proxy for sewage loads in the lakes [14], implying the urban sewage contribution of high $p\text{CO}_2$.

We found that $p\text{CO}_2$ increased as eutrophication status increased (Figure 6a). The effect of eutrophication on CO_2 was closely bound up the interaction of CO_2 consumption and production [26,52]. Previous studies have found algae blooms enabled the lake to absorb CO_2 from the atmosphere [53,54]. We, however, observed an atmospheric CO_2 source of the studied lake even in the summer season, with much higher Chl-a concentration. This implied the importance of respiration rather than photosynthesis in the eutrophic Lake Tangxun [55,56]. Thus, Lake Tangxun, a net CO_2 source, is characterized by a heterotrophic nature, supporting the positive associations between $p\text{CO}_2$ and nutrient species (Figure 5).

4.3. $d\text{CH}_4$ Control Factors

Geochemical controls of CH_4 dynamics in aquatic ecosystems are complicated [37,57]. First, CH_4 production and consumption are controlled by methanogenic and aerobic methane-oxidizing bacteria [37,58,59]. They are also affected by algae decay in eutrophic lakes [46,60,61]. Previous studies have also showed that algal blooms have a catalytic effect on CH_4 dynamics [53,62]. Second, variations in microenvironmental factors such as pH and DO can affect CH_4 production and consumption [45,63]. CH_4 is easily oxidized to carbon dioxide; thus, low DO concentration can decrease CH_4 oxidation and increase CH_4 production [64,65]. These processes led to the negative correlation between $d\text{CH}_4$ and DO (Figure 7b). The positive correlation between $d\text{CH}_4$ and $p\text{CO}_2$ (Figure 7f) can support CH_4 oxidation to CO_2 , further evidencing the association between $d\text{CH}_4$ and DO. Similar results from lakes in Northeastern China and Lake Kivu in East Africa support our findings [66,67].

It was interesting that we also found a significantly negative correlation between $d\text{CH}_4$ and pH (Figure 7a). This can be explained by the pH range of 7 to 9 in Lake Tangxun. Prior studies showed that pH ranging between 6 and 8 is the most favorable for methanogenesis, and CH_4 concentrations decline as pH values drop out of the optimal range [63]. For instance, $d\text{CH}_4$ was minimal in autumn (Figure 4c) when an average pH (8.14 ± 0.59) was outside the optimal range for CH_4 production (Figure 2d,h).

The content, availability, and redox conditions of organic carbon are the pivotal factors affecting CH_4 dynamics [46]. In this study, multiple nutrients (N-NH_4^+ , TN and TP) regulated the $d\text{CH}_4$ in Lake Tangxun (Figure 7c–e). The input of nutrients can be used as the basic substrate in methanogenesis [19,46]. Meanwhile, nitrogen input also promoted CH_4 production by providing sufficient substrate for the methanogens' growth [57,68]. N-NH_4^+ was also a good proxy for estimating $d\text{CH}_4$ in Lake Tangxun (Table 1). It proved ammonia nitrogen can prevent CH_4 oxidation [69], as reflected by the correlation between N-NH_4^+ and $d\text{CH}_4$ (Figure 7c).

Consistent with $p\text{CO}_2$, eutrophication increased $d\text{CH}_4$, as suggested by the significantly positive correlation between TSI and $d\text{CH}_4$ (Figure 6b). Several studies supported our findings [19,29,62]. Eutrophic lakes provided most labile organic matter that can be promptly converted to CH_4 precursors [28], as reflected by the positive correlation between $d\text{CH}_4$ and nutrients (Figure 7c–e). Beaulieu and DelSontro [62] also found enhanced eutrophication of lentic waters could substantially increase CH_4 emission. Meanwhile, shallow eutrophic lakes are suitable for submerged vegetation, which can also provide substrates to promote CH_4 production [70]. Moreover, Sepulveda-Jauregui and Hoyos-Santillan [71] found that eutrophic lakes had higher temperature sensitivity, resulting in higher CH_4 emission. In Lake Tangxun, in summer, the TSI and temperature were the highest, and $d\text{CH}_4$ was the highest (Figures 3 and 4c). In winter, although there was slightly higher DOC concentration than in spring and summer, the trophic status and temperature was the lowest, leading to relatively lower $d\text{CH}_4$.

4.4. Implications of CO_2 and CH_4 Flux

Urban lakes had notable spatial–temporal heterogeneity of CO_2 flux, and acted as a considerable atmospheric CO_2 source (Table 2). CO_2 flux (averaging $5.52 \text{ mmol m}^{-2} \text{ d}^{-1}$) in this study was lower than in other studies (averaging $20.80 \text{ mmol m}^{-2} \text{ d}^{-1}$) (Table 2). Sydney's severe eutrophic urban lake showed the peaking flux of CO_2 [72]. What is noteworthy is that CO_2 emissions were not only subject to lake nutrient loadings, but also controlled by seasonal variation of ambient conditions, as exhibited in recent studies in subtropical urban eutrophic lakes [54,73]. Sun et al. [19] and Zhang et al. [54] found eutrophic lakes converted to be CO_2 sinks in summer due to higher primary productivity, which was different from our results in Lake Tangxun. This implied that seasonal sampling can lead to large uncertainty of lake CO_2 emission.

Urban lakes in subtropical zones showed higher CH_4 fluxes than those in boreal zones (Table 2). This was likely due to the rate of methanogenesis and substrate production increase with a warmer temperature [74–76]. Furthermore, inputs of sewage also contributed to higher CH_4 fluxes in urban lakes, such as the severely polluted Lake Bellandur [22]. Besides the study lake ecosystem, other aquatic ecosystems in urban areas also showed higher CH_4 fluxes [5,36,77]. Rosentreter, Borges [11] also demonstrated that CH_4 emissions are likely to increase because of eutrophication and urbanization based on a metadata analysis of CH_4 fluxes in all major aquatic ecosystems. We suggest that more field measures should be conducted, to better understand CH_4 dynamics in lakes.

The eutrophication effect of GHG emissions in the urban lakes was not fully understood. Our results provided new understanding into seasonal fluctuations of CO_2 and CH_4 diffusive fluxes in a middle eutrophic urban lake. We highlighted that eutrophication could significantly promote CO_2 and CH_4 from lake into atmosphere. This is particularly evident in the eutrophic lakes of the Yangtze Basin, as supported by increasing lake CO_2 and CH_4 emissions as the trophic state increase [15,57]. Hence, the management (e.g., retreatment

of wastewater) and ecological restoration (e.g., sediment dredging) measures of lakes are necessary in highly urban-dominated regions, which could not only decrease lacustrine carbon emission in urban lakes, but also improve water quality, further contributing to the goal of carbon neutrality.

Table 2. CO₂ and CH₄ diffusive fluxes in others urban lakes in different climate zones.

Lake	City	Climate Zone	Sampling Time	FCO ₂ (mmol m ⁻² d ⁻¹)	FCH ₄ (mmol m ⁻² d ⁻¹)	Source
Lake Vesijärvi	Finland	Boreal	May–October 2018	12.4 ± 2.38	0.24 ± 0.06	[24]
Lake Obersee, et al.	Berlin	Temperate	April–May and July–October 2016, February–March 2017		2.19	[76]
Sydney’s largest urban lake	Sydney	Temperate	June and July 2019	113 ± 81	0.3 ± 0.1	[72]
Lake Lyng	Silkeborg	Temperate	September–October 2021	22.05	1.68	[78]
Lake SCH and YYT	Beijing	Temperate	July 2018–November 2019	−0.2 ± 13.0	0.7 ± 0.6	[79]
Lake Wuli	Wuxi	Subtropic	2000–2015	25.0 ± 13.64		[14]
			2002–2017	21.12 ± 19.60		[15]
Lake Donghu	Wuhan	Subtropic	April 2003–March 2004	7.7	1.6	[45]
			2002–2017	16.42 ± 20.39		[15]
Lake Nanhu, et al.	Wuhan	Subtropic	October–December 2021, February–March and May–June 2022	3.65	1.32 ± 4.11	[54,57]
Lake Tangxun	Wuhan	Subtropic	October 2022, February, April and June 2023	5.52 ± 12.16	0.83 ± 2.81	This study
Lake Bhalswa	Dehli	Tropic	Summer 2018	11.65 ± 3.42		[80]
			Winter 2017	6.33 ± 2.23		
Lake Bellandur	Bangalore	Tropic	June 2018–February 2020	5.81	3.6	[22]
Lake Jakkur	Bangalore	Tropic	June 2018–February 2020	4.5	1.48	[22]

5. Conclusions

The study investigated the seasonal dynamics and potential control factors of dissolved CO₂ and CH₄ in the largest Chinese urban Lake. Our results illustrated that Lake Tangxun was atmospheric greenhouse gases (GHGs) source. CO₂ and CH₄ concentrations and thus diffusion fluxes significantly increased as trophic status index increased. We further found that N-NH₄⁺ was a predictor of *p*CO₂ and *d*CH₄. More studies should be conducted to accurately quantify carbon emission in eutrophic lakes, particularly in urban areas that are intensively affected by human activities. The study highlighted the importance of eutrophic control for restoration of water environment and reducing CO₂ and CH₄ emissions. Meanwhile, this study also stressed that urban lakes, which are heavily influenced by human activities, exhibited more complex seasonal dynamics in CO₂ and CH₄ fluxes. Therefore, urban lakes should be considered an important component of carbon budgets.

Supplementary Materials: The following supporting information can be downloaded at: <https://www.mdpi.com/article/10.3390/w16010136/s1>, Figure S1: Air Temperature (°C) and precipitation (mm) from August 2022 to July 2023; Figure S2: The relationship between the *p*CO₂ and (a) T_a; (b) precipitation; Figure S3: The relationship between the GHG emission and *U*: (a) CO₂ emission; (b) CH₄ emission; Table S1: Water quality parameters of sampling sites in Lake Tangxun Table S2: Relationships between dissolved partial pressure of CO₂ (*p*CO₂), diffusive fluxes (FCO₂), dissolved CH₄ (*d*CH₄), diffusive fluxes (FCH₄) and water environmental parameters. All the data used Spearman correlation analysis.

Author Contributions: Conceptualization, S.L.; methodology, B.M. and S.L.; software, B.M.; validation, B.M.; formal analysis, B.M.; investigation, B.M., Y.W. and P.J.; data curation, B.M. and Y.W.; writing—original draft preparation, B.M.; writing—review and editing, S.L.; visualization, B.M., S.L. and Y.W.; supervision, S.L.; project administration, S.L. All authors have read and agreed to the published version of the manuscript.

Funding: This research was funded by the National Natural Science Foundation of China (32102823), Wuhan Institute of Technology to Siyue Li (21QD02).

Data Availability Statement: The data presented in this study are available in supplementary material.

Acknowledgments: We are grateful to Yunting Han, Shiwang Ma, Yanyu Zhong and Jingquan Le for their outstanding assistance in the field.

Conflicts of Interest: The authors declare no conflict of interest. Siyue Li would like to declare on behalf of the co-authors that the work described was original research that has not been published previously, and is not under consideration for publication elsewhere, in whole or in part.

References

1. Tranvik, L.J.; Downing, J.A.; Cotner, J.B.; Loiselle, S.A.; Striegl, R.G.; Ballatore, T.J.; Dillon, P.; Finlay, K.; Fortino, K.; Knoll, L.B.; et al. Lakes and reservoirs as regulators of carbon cycling and climate. *Limnol. Oceanogr.* **2009**, *54*, 2298–2314. [[CrossRef](#)]
2. Cole, J.J.; Prairie, Y.T.; Caraco, N.F.; McDowell, W.H.; Tranvik, L.J.; Striegl, R.G.; Duarte, C.M.; Kortelainen, P.; Downing, J.A.; Middelburg, J.J.; et al. Plumbing the Global Carbon Cycle: Integrating Inland Waters into the Terrestrial Carbon Budget. *Ecosystems* **2007**, *10*, 172–185. [[CrossRef](#)]
3. Regnier, P.; Friedlingstein, P.; Ciais, P.; Mackenzie, F.T.; Gruber, N.; Janssens, I.A.; Laruelle, G.G.; Lauerwald, R.; Luysaert, S.; Andersson, A.J.; et al. Anthropogenic perturbation of the carbon fluxes from land to ocean. *Nat. Geosci.* **2013**, *6*, 597–607. [[CrossRef](#)]
4. Li, Y.; Shang, J.; Zhang, C.; Zhang, W.; Niu, L.; Wang, L.; Zhang, H. The role of freshwater eutrophication in greenhouse gas emissions: A review. *Sci. Total Environ.* **2021**, *768*, 144582. [[CrossRef](#)]
5. Pilla, R.M.; Griffiths, N.A.; Gu, L.; Kao, S.C.; McManamay, R.; Ricciuto, D.M.; Shi, X. Anthropogenically driven climate and landscape change effects on inland water carbon dynamics: What have we learned and where are we going? *Glob. Chang. Biol.* **2022**, *28*, 5601–5629. [[CrossRef](#)] [[PubMed](#)]
6. Holgerson, M.A.; Raymond, P.A. Large contribution to inland water CO₂ and CH₄ emissions from very small ponds. *Nat. Geosci.* **2016**, *9*, 222–226. [[CrossRef](#)]
7. Borges, A.V.; Darchambeau, F.; Teodoru, C.R.; Marwick, T.R.; Tamooh, F.; Geeraert, N.; Omengo, F.O.; Guérin, F.; Lambert, T.; Morana, C.; et al. Globally significant greenhouse-gas emissions from African inland waters. *Nat. Geosci.* **2015**, *8*, 637–642. [[CrossRef](#)]
8. Johnson, M.S.; Matthews, E.; Du, J.; Genovese, V.; Bastviken, D. Methane Emission from Global Lakes: New Spatiotemporal Data and Observation-Driven Modeling of Methane Dynamics Indicates Lower Emissions. *J. Geophys. Res.* **2022**, *127*, e2022JG006793. [[CrossRef](#)]
9. Bastviken, D.; Cole, J.; Pace, M.; Tranvik, L. Methane emissions from lakes: Dependence of lake characteristics, two regional assessments, and a global estimate. *Glob. Biogeochem. Cycles* **2004**, *18*, GB4009. [[CrossRef](#)]
10. Bastviken, D.; Tranvik, L.J.; Downing, J.A.; Crill, P.M.; Enrich-Prast, A. Freshwater Methane Emissions Offset the Continental Carbon Sink. *Science* **2011**, *331*, 50–51. [[CrossRef](#)]
11. Rosentreter, J.A.; Borges, A.V.; Deemer, B.R.; Holgerson, M.A.; Liu, S.; Song, C.; Melack, J.; Raymond, P.A.; Duarte, C.M.; Allen, G.H.; et al. Half of global methane emissions come from highly variable aquatic ecosystem sources. *Nat. Geosci.* **2021**, *14*, 225–230. [[CrossRef](#)]
12. Downing, J.A.; Prairie, Y.T.; Cole, J.J.; Duarte, C.M.; Tranvik, L.J.; Striegl, R.G.; McDowell, W.H.; Kortelainen, P.; Caraco, N.F.; Melack, J.M.; et al. The global abundance and size distribution of lakes, ponds, and impoundments. *Limnol. Oceanogr.* **2006**, *51*, 2388–2397. [[CrossRef](#)]
13. Birch, S.; McCaskie, J. Shallow urban lakes a challenge for lake management. *Hydrobiologia* **1999**, *395*, 365–377. [[CrossRef](#)]
14. Xiao, Q.; Duan, H.; Qi, T.; Hu, Z.; Liu, S.; Zhang, M.; Lee, X. Environmental investments decreased partial pressure of CO₂ in a small eutrophic urban lake: Evidence from long-term measurements. *Environ. Pollut.* **2020**, *263*, 114433. [[CrossRef](#)] [[PubMed](#)]
15. Xiao, Q.; Xiao, W.; Luo, J.; Qiu, Y.; Hu, C.; Zhang, M.; Qi, T.; Duan, H. Management actions mitigate the risk of carbon dioxide emissions from urban lakes. *J. Environ. Manag.* **2023**, *344*, 118626. [[CrossRef](#)]
16. Colina, M.; Kosten, S.; Silvera, N.; Clemente, J.M.; Meerhoff, M. Carbon fluxes in subtropical shallow lakes: Contrasting regimes differ in CH₄ emissions. *Hydrobiologia* **2021**, *849*, 3813–3830. [[CrossRef](#)]
17. Martinez-Cruz, K.; Gonzalez-Valencia, R.; Sepulveda-Jauregui, A.; Plascencia-Hernandez, F.; Belmonte-Izquierdo, Y.; Thalasso, F. Methane emission from aquatic ecosystems of Mexico City. *Aquat. Sci.* **2016**, *79*, 159–169. [[CrossRef](#)]
18. Xiao, Q.; Duan, H.; Qin, B.; Hu, Z.; Zhang, M.; Qi, T.; Lee, X. Eutrophication and temperature drive large variability in carbon dioxide from China's Lake Taihu. *Limnol. Oceanogr.* **2021**, *67*, 379–391. [[CrossRef](#)]
19. Sun, H.; Lu, X.; Yu, R.; Yang, J.; Liu, X.; Cao, Z.; Zhang, Z.; Li, M.; Geng, Y. Eutrophication decreased CO₂ but increased CH₄ emissions from lake: A case study of a shallow Lake Ulansuhai. *Water Res.* **2021**, *201*, 117363. [[CrossRef](#)]
20. Holgerson, M.A.; Richardson, D.C.; Roith, J.; Bortolotti, L.E.; Finlay, K.; Hornbach, D.J.; Gurung, K.; Ness, A.; Andersen, M.R.; Bansal, S.; et al. Classifying Mixing Regimes in Ponds and Shallow Lakes. *Water Resour. Res.* **2022**, *58*, e2022WR032522. [[CrossRef](#)]

21. Zhu, L.; Qin, B.; Zhou, J.; Van Dam, B.; Shi, W. Effects of turbulence on carbon emission in shallow lakes. *J. Environ. Sci.* **2018**, *69*, 166–172. [[CrossRef](#)]
22. Pickard, A.; White, S.; Bhattacharyya, S.; Carvalho, L.; Dobel, A.; Drewer, J.; Jamwal, P.; Helfter, C. Greenhouse gas budgets of severely polluted urban lakes in India. *Sci. Total Environ.* **2021**, *798*, 149019. [[CrossRef](#)] [[PubMed](#)]
23. Zhao, Z.; Zhang, D.; Shi, W.; Ruan, X.; Sun, J. Understanding the Spatial Heterogeneity of CO₂ and CH₄ Fluxes from an Urban Shallow Lake: Correlations with Environmental Factors. *J. Chem.* **2017**, *2017*, 8175631. [[CrossRef](#)]
24. López Bellido, J.; Peltomaa, E.; Ojala, A. An urban boreal lake basin as a source of CO₂ and CH₄. *Environ. Pollut.* **2011**, *159*, 1649–1659. [[CrossRef](#)]
25. Andrade, C.; Cruz, J.V.; Viveiros, F.; Coutinho, R. Diffuse CO₂ emissions from Sete Cidades volcanic lake (São Miguel Island, Azores): Influence of eutrophication processes. *Environ. Pollut.* **2021**, *268*, 115624. [[CrossRef](#)] [[PubMed](#)]
26. Xiao, Q.; Xu, X.; Duan, H.; Qi, T.; Qin, B.; Lee, X.; Hu, Z.; Wang, W.; Xiao, W.; Zhang, M. Eutrophic Lake Taihu as a significant CO₂ source during 2000–2015. *Water Res.* **2020**, *170*, 115331. [[CrossRef](#)] [[PubMed](#)]
27. Zhou, J.; Leavitt, P.R.; Zhang, Y.; Qin, B. Anthropogenic eutrophication of shallow lakes: Is it occasional? *Water Res.* **2022**, *221*, 118728. [[CrossRef](#)]
28. Davidson, T.A.; Audet, J.; Jeppesen, E.; Landkildehus, F.; Lauridsen, T.L.; Søndergaard, M.; Syväranta, J. Synergy between nutrients and warming enhances methane ebullition from experimental lakes. *Nat. Clim. Chang.* **2018**, *8*, 156–160. [[CrossRef](#)]
29. DelSontro, T.; Beaulieu, J.J.; Downing, J.A. Greenhouse gas emissions from lakes and impoundments: Upscaling in the face of global change. *Limnol. Oceanogr. Lett.* **2018**, *3*, 64–75. [[CrossRef](#)]
30. Balmer, M.; Downing, J. Carbon dioxide concentrations in eutrophic lakes: Undersaturation implies atmospheric uptake. *Inland Waters* **2011**, *1*, 125–132. [[CrossRef](#)]
31. Yang, W.; Xu, M.; Li, R.; Zhang, L.; Deng, Q. Estimating the ecological water levels of shallow lakes: A case study in Tangxun Lake, China. *Sci. Rep.* **2020**, *10*, 5637. [[CrossRef](#)] [[PubMed](#)]
32. Yao, K.; Xie, Z.; Zhi, L.; Wang, Z.; Qu, C. Polycyclic Aromatic Hydrocarbons in the Water Bodies of Dong Lake and Tangxun Lake, China: Spatial Distribution, Potential Sources and Risk Assessment. *Water* **2023**, *15*, 2416. [[CrossRef](#)]
33. Yang, J. Study on Lake's Dynamic Assimilative Capacity Based on Two-Dimensional Hydrodynamic and Water Quality Simulation. Ph.D. Thesis, Huazhong University of Science and Technology, Wuhan, China, 2020.
34. Wang, G.; Liu, S.; Sun, S.; Xia, X. Unexpected low CO₂ emission from highly disturbed urban inland waters. *Environ. Res.* **2023**, *235*, 116689. [[CrossRef](#)] [[PubMed](#)]
35. Zhang, W.; Li, H.; Xiao, Q.; Li, X. Urban rivers are hotspots of riverine greenhouse gas (N₂O, CH₄, CO₂) emissions in the mixed-landscape chaohu lake basin. *Water Res.* **2021**, *189*, 116624. [[CrossRef](#)] [[PubMed](#)]
36. Tang, W.; Xu, Y.J.; Ni, M.; Li, S. Land use and hydrological factors control concentrations and diffusive fluxes of riverine dissolved carbon dioxide and methane in low-order streams. *Water Res.* **2023**, *231*, 119615. [[CrossRef](#)] [[PubMed](#)]
37. Tang, W.; Xu, Y.J.; Ma, Y.; Maher, D.T.; Li, S. Hot spot of CH₄ production and diffusive flux in rivers with high urbanization. *Water Res.* **2021**, *204*, 117624. [[CrossRef](#)] [[PubMed](#)]
38. Cole, J.J.; Caraco, N.F. Atmospheric exchange of carbon dioxide in a low-wind oligotrophic lake measured by the addition of SF₆. *Limnol. Oceanogr.* **1998**, *43*, 647–656. [[CrossRef](#)]
39. Crusius, J.; Wanninkhof, R. Gas transfer velocities measured at low wind speed over a lake. *Limnol. Oceanogr.* **2003**, *48*, 1010–1017. [[CrossRef](#)]
40. Hope, D.; Palmer, S.M.; Billett, M.F.; Dawson, J.J.C. Variations in dissolved CO₂ and CH₄ in a first-order stream and catchment: An investigation of soil-stream linkages. *Hydrol. Process.* **2004**, *18*, 3255–3275. [[CrossRef](#)]
41. Yang, R.; Xu, Z.; Liu, S.; Xu, Y.J. Daily pCO₂ and CO₂ flux variations in a subtropical mesotrophic shallow lake. *Water Res.* **2019**, *153*, 29–38. [[CrossRef](#)]
42. Davidson, E.A.; Figueiredo, R.O.; Markewitz, D.; Aufdenkampe, A.K. Dissolved CO₂ in small catchment streams of eastern Amazonia: A minor pathway of terrestrial carbon loss. *J. Geophys. Res.* **2010**, *115*, G04005. [[CrossRef](#)]
43. Wang, X.; He, Y.; Yuan, X.; Chen, H.; Peng, C.; Zhu, Q.; Yue, J.; Ren, H.; Deng, W.; Liu, H. pCO₂ and CO₂ fluxes of the metropolitan river network in relation to the urbanization of Chongqing, China. *J. Geophys. Res.* **2017**, *122*, 470–486. [[CrossRef](#)]
44. Wang, X.; Yu, L.; Liu, T.; He, Y.; Wu, S.; Chen, H.; Yuan, X.; Wang, J.; Li, X.; Li, H.; et al. Methane and nitrous oxide concentrations and fluxes from heavily polluted urban streams: Comprehensive influence of pollution and restoration. *Environ. Pollut.* **2022**, *313*, 120098. [[CrossRef](#)] [[PubMed](#)]
45. Xing, Y.; Xie, P.; Yang, H.; Ni, L.; Wang, Y.; Rong, K. Methane and carbon dioxide fluxes from a shallow hypereutrophic subtropical Lake in China. *Atmos. Environ.* **2005**, *39*, 5532–5540. [[CrossRef](#)]
46. Zhou, Y.; Song, K.; Han, R.; Riya, S.; Xu, X.; Yeerken, S.; Geng, S.; Ma, Y.; Terada, A. Nonlinear response of methane release to increased trophic state levels coupled with microbial processes in shallow lakes. *Environ. Pollut.* **2020**, *265*, 114919. [[CrossRef](#)] [[PubMed](#)]
47. Zhu, Y.; Purdy, K.J.; Eyice, Ö.; Shen, L.; Harpenslager, S.F.; Yvon-Durocher, G.; Dumbrell, A.J.; Trimmer, M. Disproportionate increase in freshwater methane. *Nat. Clim. Chang.* **2020**, *10*, 685–690. [[CrossRef](#)]
48. Natchimuthu, S.; Sundgren, I.; Gålfalk, M.; Klemedtsson, L.; Crill, P.; Danielsson, Å.; Bastviken, D. Spatio-temporal variability of lake CH₄ fluxes and its influence on annual whole lake emission estimates. *Limnol. Oceanogr.* **2015**, *61*, S13–S26. [[CrossRef](#)]

49. Li, Y.; Zhou, Y.; Zhou, L.; Zhang, Y.; Xu, H.; Jang, K.-S.; Kothawala, D.N.; Spencer, R.G.M.; Jeppesen, E.; Brookes, J.D.; et al. Changes in Water Chemistry Associated with Rainstorm Events Increase Carbon Emissions from the Inflowing River Mouth of a Major Drinking Water Reservoir. *Environ. Sci. Technol.* **2022**, *56*, 16494–16505. [[CrossRef](#)]
50. Chan, C.N.; Bogard, M.J.; Ma, F.C.; Ip, Y.C.; Liu, B.; Chen, S.; Ran, L. CO₂ dynamics in a small and old subtropical reservoir in East Asia: Environmental controls driving seasonal and spatial variability. *Sci. Total Environ.* **2023**, *856*, 159047. [[CrossRef](#)]
51. Yuan, D.; Xu, Y.J.; Ma, S.; Le, J.; Zhang, K.; Miao, R.; Li, S. Nitrogen addition effect overrides warming effect on dissolved CO₂ and phytoplankton structure in shallow lakes. *Water Res.* **2023**, *244*, 120437. [[CrossRef](#)]
52. Perga, M.-E.; Maberly, S.C.; Jenny, J.-P.; Alric, B.; Pignol, C.; Naffrechoux, E. A century of human-driven changes in the carbon dioxide concentration of lakes. *Glob. Biogeochem. Cycles* **2016**, *30*, 93–104. [[CrossRef](#)]
53. Zhang, L.; He, K.; Wang, T.; Liu, C.; An, Y.; Zhong, J. Frequent algal blooms dramatically increase methane while decrease carbon dioxide in a shallow lake bay. *Environ. Pollut.* **2022**, *312*, 120061. [[CrossRef](#)] [[PubMed](#)]
54. Zhang, L.; Xu, Y.J.; Li, S. Changes in CO₂ concentration and degassing of eutrophic urban lakes associated with algal growth and decline. *Environ. Res.* **2023**, *237*, 117031. [[CrossRef](#)] [[PubMed](#)]
55. Davidson, T.A.; Audet, J.; Svenning, J.-C.; Lauridsen, T.L.; Søndergaard, M.; Landkildehus, F.; Larsen, S.E.; Jeppesen, E. Eutrophication effects on greenhouse gas fluxes from shallow-lake mesocosms override those of climate warming. *Glob. Chang. Biol.* **2015**, *21*, 4449–4463. [[CrossRef](#)] [[PubMed](#)]
56. Morales-Williams, A.M.; Wanamaker, A.D.; Williams, C.J.; Downing, J.A. Eutrophication Drives Extreme Seasonal CO₂ Flux in Lake Ecosystems. *Ecosystems* **2020**, *24*, 434–450. [[CrossRef](#)]
57. Zhang, L.; Xu, Y.J.; Ma, B.; Jiang, P.; Li, S. Intense methane diffusive emissions in eutrophic urban lakes, Central China. *Environ. Res.* **2023**, *237*, 117073. [[CrossRef](#)] [[PubMed](#)]
58. Shelley, F.; Abdullahi, F.; Grey, J.; Trimmer, M. Microbial methane cycling in the bed of a chalk river: Oxidation has the potential to match methanogenesis enhanced by warming. *Freshw. Biol.* **2015**, *60*, 150–160. [[CrossRef](#)]
59. Stanley, E.H.; Casson, N.J.; Christel, S.T.; Crawford, J.T.; Loken, L.C.; Oliver, S.K. The ecology of methane in streams and rivers patterns, controls, and global significance. *Ecol. Monogr.* **2016**, *86*, 146–171. [[CrossRef](#)]
60. Yan, X.; Xu, X.; Ji, M.; Zhang, Z.; Wang, M.; Wu, S.; Wang, G.; Zhang, C.; Liu, H. Cyanobacteria blooms: A neglected facilitator of CH₄ production in eutrophic lakes. *Sci. Total Environ.* **2019**, *651*, 466–474. [[CrossRef](#)]
61. Yan, X.; Xu, X.; Wang, M.; Wang, G.; Wu, S.; Li, Z.; Sun, H.; Shi, A.; Yang, Y. Climate warming and cyanobacteria blooms: Looks at their relationships from a new perspective. *Water Res.* **2017**, *125*, 449–457. [[CrossRef](#)]
62. Beaulieu, J.J.; DelSontro, T.; Downing, J.A. Eutrophication will increase methane emissions from lakes and impoundments during the 21st century. *Nat. Commun.* **2019**, *10*, 1375. [[CrossRef](#)] [[PubMed](#)]
63. Yang, P.; Zhang, Y.; Yang, H.; Zhang, Y.; Xu, J.; Tan, L.; Tong, C.; Lai, D.Y.F. Large Fine-Scale Spatiotemporal Variations of CH₄ Diffusive Fluxes from Shrimp Aquaculture Ponds Affected by Organic Matter Supply and Aeration in Southeast China. *J. Geophys. Res.* **2019**, *124*, 1290–1307. [[CrossRef](#)]
64. Ivanov, M.V.; Pimenov, N.V.; Rusanov, I.I.; Lein, A.Y. Microbial Processes of the Methane Cycle at the North-western Shelf of the Black Sea. *Estuar. Coast. Shelf Sci.* **2002**, *54*, 589–599. [[CrossRef](#)]
65. Hu, B.; Wang, D.; Zhou, J.; Meng, W.; Li, C.; Sun, Z.; Guo, X.; Wang, Z. Greenhouse gases emission from the sewage draining rivers. *Sci. Total Environ.* **2018**, *612*, 1454–1462. [[CrossRef](#)] [[PubMed](#)]
66. Wen, Z.; Song, K.; Zhao, Y.; Jin, X. Carbon dioxide and methane supersaturation in lakes of semi-humid/semi-arid region, Northeastern China. *Atmos. Environ.* **2016**, *138*, 65–73. [[CrossRef](#)]
67. Gomez-Gesteira, M.; Borges, A.V.; Morana, C.; Bouillon, S.; Servais, P.; Descy, J.-P.; Darchambeau, F. Carbon Cycling of Lake Kivu (East Africa): Net Autotrophy in the Epilimnion and Emission of CO₂ to the Atmosphere Sustained by Geogenic Inputs. *PLoS ONE* **2014**, *9*, e109500.
68. Wang, B.; Stirling, E.; He, Z.; Ma, B.; Zhang, H.; Zheng, X.; Xiao, F.; Yan, Q. Pollution alters methanogenic and methanotrophic communities and increases dissolved methane in small ponds. *Sci. Total Environ.* **2021**, *801*, 149723. [[CrossRef](#)]
69. Bodelier, P.L.E.; Laanbroek, H.J. Nitrogen as a regulatory factor of methane oxidation in soils and sediments. *FEMS Microbiol. Ecol.* **2004**, *47*, 265–277. [[CrossRef](#)]
70. Xiao, Q.; Zhang, M.; Hu, Z.; Gao, Y.; Hu, C.; Liu, C.; Liu, S.; Zhang, Z.; Zhao, J.; Xiao, W.; et al. Spatial variations of methane emissiodn in a large shallow eutrophic lake in subtropical climate. *J. Geophys. Res.* **2017**, *122*, 1597–1614. [[CrossRef](#)]
71. Sepulveda-Jauregui, A.; Hoyos-Santillan, J.; Martinez-Cruz, K.; Walter Anthony, K.M.; Casper, P.; Belmonte-Izquierdo, Y.; Thalasso, F. Eutrophication exacerbates the impact of climate warming on lake methane emission. *Sci. Total Environ.* **2018**, *636*, 411–419. [[CrossRef](#)]
72. Sadat-Noori, M.; Rutledge, H.; Andersen, M.S.; Glamore, W. Quantifying groundwater carbon dioxide and methane fluxes to an urban freshwater lake using radon measurements. *Sci. Total Environ.* **2021**, *797*, 149184. [[CrossRef](#)] [[PubMed](#)]
73. Xu, Y.J.; Xu, Z.; Yang, R. Rapid daily change in surface water pCO₂ and CO₂ evasion: A case study in a subtropical eutrophic lake in Southern USA. *J. Hydrol.* **2019**, *570*, 486–494. [[CrossRef](#)]
74. Borrel, G.; Jézéquel, D.; Biderre-Petit, C.; Morel-Desrosiers, N.; Morel, J.-P.; Peyret, P.; Fonty, G.; Lehours, A.-C. Production and consumption of methane in freshwater lake ecosystems. *Res. Microbiol.* **2011**, *162*, 832–847. [[CrossRef](#)] [[PubMed](#)]

75. Fusé, V.S.; Priano, M.E.; Williams, K.E.; Gere, J.I.; Guzmán, S.A.; Gratton, R.; Juliarena, M.P. Temporal variation in methane emissions in a shallow lake at a southern mid latitude during high and low rainfall periods. *Environ. Monit. Assess.* **2016**, *188*, 590. [[CrossRef](#)] [[PubMed](#)]
76. Herrero Ortega, S.; Romero González-Quijano, C.; Casper, P.; Singer, G.A.; Gessner, M.O. Methane emissions from contrasting urban freshwaters: Rates, drivers, and a whole-city footprint. *Glob. Chang. Biol.* **2019**, *25*, 4234–4243. [[CrossRef](#)]
77. Gu, S.; Li, S.; Santos, I.R. Anthropogenic land use substantially increases riverine CO₂ emissions. *J. Environ. Sci.* **2022**, *118*, 158–170. [[CrossRef](#)]
78. Sø, J.S.; Sand-Jensen, K.; Martinsen, K.T.; Polauke, E.; Kjær, J.E.; Reitzel, K.; Kragh, T. Methane and carbon dioxide fluxes at high spatiotemporal resolution from a small temperate lake. *Sci. Total Environ.* **2023**, *878*, 162895. [[CrossRef](#)]
79. Wang, G.; Xia, X.; Liu, S.; Zhang, L.; Zhang, S.; Wang, J.; Xi, N.; Zhang, Q. Intense methane ebullition from urban inland waters and its significant contribution to greenhouse gas emissions. *Water Res.* **2021**, *189*, 116654. [[CrossRef](#)]
80. Joshi, P.; Siddaiah, N.S. Carbon dioxide dynamics of Bhalswa Lake: A human-impacted urban wetland of Delhi, India. *Environ. Dev. Sustain.* **2021**, *23*, 18116–18142. [[CrossRef](#)]

Disclaimer/Publisher’s Note: The statements, opinions and data contained in all publications are solely those of the individual author(s) and contributor(s) and not of MDPI and/or the editor(s). MDPI and/or the editor(s) disclaim responsibility for any injury to people or property resulting from any ideas, methods, instructions or products referred to in the content.